

ADSORPTION OF DYES BY MESOPOROUS CARBON (CMK-1)

KISWANTO^{1,2}, HANGGARA SUDRAJAT^{2*}, SHEILA LI¹, PEN SATHYAVISAL³ and ANGELA C. NGAH⁴

¹School of Chemistry, University of Wollongong, Wollongong NSW 2522, Australia

²Faculty of Biology, Gadjah Mada University, Yogyakarta 55281, Indonesia

³Department of Chemistry, Royal University of Phnom Penh, Phnom Penh 413, Cambodia

⁴IFS, Massey University Auckland, Private Bag 102904, Auckland, New Zealand

*Corresponding author: Phone: +62 858 68077123; Fax: +62 274 546187, E-mail: angga_vanniveau@yahoo.co.id

Received: 5th January 2009; Revised: 14th February 2009; Accepted: 14th February 2009

Abstract: This work deals with dye adsorption using mesoporous carbon (CMK-1) as the adsorbent in addition to activated carbon (Norit SX22). CMK-1 was synthesized using mesoporous silica (MCM-48) as a template and sucrose as a carbon source. Sulphuric acid was utilized as a catalyst in carbonization process. Adsorbates used were reactive (reactive red-1, RR1), basic (Rhodamine B, RhB), and acid (Patent Blue V, PBV) dyes. The optimum contact time of dyes with CMK-1 was 120 min. The adsorption of the dyes in CMK-1 and activated carbon can be fitted to both the Langmuir and Freundlich models. The adsorption of the dyes using CMK-1 was considerable higher than that using Norit SX2. The amount of dyes adsorbed by CMK-1 was in the order of RR1 > RhB > PBV.

Keywords: Adsorption, dyes, mesoporous carbon

INTRODUCTION

Dyes are group of substances used widely in industries. These substances cause problems in an aquatic environment. Water containing dyes cannot be accepted for drinking water or for agricultural purposes due to aesthetical reason. Dyes affect the characteristic of water because they protect sunlight penetration leading to decrease photosynthetic processes. Some dyes are carcinogenic and mutagenic. Therefore, dyes need to be removed from wastewater before mixing with the clean water. Among industrial wastewaters, dye containing wastewater from textile and dyestuff industries is the most difficult to treat. This is because dyes usually have a synthetic origin and complex aromatic molecular structures, which make them more stable and more difficult to be biodegraded [1]. As a consequence, dyes cannot be treated by a conventional method, i.e. aerobic degradation.

Adsorption is an effective method for lowering the concentration of such materials in the environment, especially if the adsorbent has high adsorption capacity. In this regard, activated

carbon has been evaluated extensively for the waste treatment of the different classes of dyes [2-4]. Unfortunately, this material generally has micro pore size and as a result, its adsorption capacity to big molecule is small. The synthesis of mesoporous carbon called CMK-1 exhibiting highly ordered X-ray powder diffraction (XRD) pattern was reported [5]. Since its discovery, studies of CMK-1 were mostly focused on characterization. Some studies on adsorption of small molecule in gas phase, such as N₂, Ar, and benzene have been performed [6]. Results showed that CMK-1 had capability to adsorb such materials. Vinu, *et al.* [7] reported the use of CMK-3 for adsorption of L-histidine. However, the use of CMK-1 to adsorb dyes has not been published.

This work deals with dye adsorption using mesoporous carbon (CMK-1) as the adsorbent. For comparison, activated carbon (Norit SX2) was used. The template MCM-48 was also tested for the adsorption of dyes. The objective of the study is find out the ability of CMK-1 in adsorbing dyes from their solution. Data obtained can be use as a basic consideration in treating wastewater contaminated by dyes.

MATERIALS AND METHODS

Material s

Materials used in this study were colloidal silica Ludox HS40 (39.5 wt% SiO₂, 0.4 wt% Na₂O and 60.1 wt% H₂O, Du Pont), 1 M sodium hydroxide, cethyltrimethylammonium bromide (CTAB; Aldrich), Triton X-100 (Sigma), sucrose (Merck), concentrated sulphuric acid (Merck), 2.5 wt% sodium hydroxide in 50% ethanol, Reactive Red 1, Rhodamine B, and Patent Blue V.

Equipment

A Siemens D500 diffractometer using CuK α ($\lambda = 1.5412 \text{ \AA}$) as a radiation source was used to obtain XRD patterns. The diffractometer was interfaced to a PC computer and the operating software used was Sietronic SIE 122D. A Micromeritics AccuSorb model 2100D was used to obtain the adsorption isotherm and the surface area of samples. A microbalance (MK2 model from C.I Electronic Limited), connected to the vacuum system was utilized to study adsorption of water and benzene. A Varian Cary 100 UV-Visible Spectrophotometer was used to analyze the amount of dyes adsorbed in mesoporous carbon and activated carbon.

Synthesis of MCM-48

Silicate solution was prepared by mixing 14.3 g of Ludox HS40 solution with 45.25 g of 1 M aqueous NaOH solution. The surfactant mixture was prepared by dissolving 6.12 g of CTAB and 1.34 g of Triton X-100 simultaneously in 83.47 g of distilled water with heating. After cooling the sodium tetrasilicate solution and the surfactant solution to room temperature, both solutions were mixed quickly in a large polypropylene bottle. The bottle was immediately capped and shaken vigorously. The gel mixture obtained was heated under static condition at 373 K for 24 h. At this stage, the surfactant-silica mesophases were formed. To avoid separation of the mesophases at an early stage of heating, the bottle containing the mixture was sometimes agitated. The reaction mixture was then cooled to room temperature and acetic acid (30 wt%) was added subsequently into the mixture in order to adjust the pH to 10. After the pH adjustment, the mixture was heated again at 373 K for 24 h and cooled to room temperature. 2.95 g of NaCl was added into the mixture and the mixture was heated at 373 K for 1 more day. As-synthesized MCM-48 was then filtered, washed with doubly distilled water and dried at 393 K in an oven. The surfactant was removed from the white product by washing with HCl-ethanol mixture; 1 g of MCM-48 was washed with 25 mL of 0.1 M HCl in 50 % aqueous ethanol solution. The precipitate was calcined

in air under static condition in a muffle furnace. The temperature was raised from room temperature to 823 K at a ramp rate of 1 K min⁻¹ and maintained at 823 K for 18 h.

Synthesis of Mesoporous Carbon (CMK-1)

One gram of dehydrated MCM-48, synthesized following the above procedure, was mixed with an aqueous solution prepared from 1.25 g of sucrose, 0.07 g of sulphuric acid, H₂SO₄ and 3.0 g of H₂O in a petri dish. The mixture was put in the oven at 373 K for 1 h and the temperature was subsequently increased to 433 K and maintained at that temperature for 30 min. The sucrose was partially decomposed by this treatment. After being heating at 433 K, the product was mixed again with aqueous solution containing 0.75 g of sucrose, 0.02 g of H₂SO₄ and 2.8 g of water. The mixture was then dried in the oven with the same condition as before. After heating in the oven, the powder was heated in a quartz tube at 1173 K under flowing nitrogen gas for 3 h. The product, carbon-silica composite, was washed with 2.5 wt% of NaOH solution dissolved in 50 v/v % aqueous ethanol solution in order to remove the silica framework. 1 g of the carbon-silica composite was mixed with 60 mL of the NaOH solution and refluxed for 1.5 h at the boiling point of the solution. After that, the mixture was filtered and the refluxing procedure was repeated. The product of mesoporous carbon was then filtered, washed with 1:1 water-ethanol until the pH of the filtrate was 7 and dried.

Adsorption of Dyes in CMK-1 and Activated Carbon

About 100 mg of mesoporous carbon was weighed and activated at 393 K in the oven for 4 h. The sample was cooled to room temperature in the desiccator. Fifty mL of 300 mg L⁻¹ dye solution was added into a beaker containing the sample and stirred at room temperature using a magnetic stirrer for different period of time. These experiments were carried out in order to obtain the optimum time for adsorption monitored by UV-Vis spectrophotometer. The adsorption experiments were repeated using different concentration of dyes and stirred for certain time (optimum time). After adsorption, the solid was separated from the solution by filtering and then the UV-Vis spectrophotometer was used to determine the quantity of adsorbed dyes at an appropriate wavelength (λ_{maximum}), depending on type of dyes used as adsorbates. The amount adsorbed per g of adsorbent calculated using the following equation [1]:

$$W = \frac{(C_0 - C_e) V}{W_a} \times 1000 \quad (1)$$

where W = amount of dyes adsorbed (mg g⁻¹), C₀ = concentration of surfactant solution before adsorption, C_e = concentration of surfactant solution at equilibrium state, V = volume of surfactant solution (L), W_a = amount of adsorbent (g).

RESULTS AND DISCUSSION

Characterization

XRD patterns of mesoporous carbon and its silica template are illustrated in Figure 1. The XRD pattern results are in agreement with those reported in previous work [5]. It can be seen that there is a systematic transformation of structure during the removal of silica framework of MCM-48 after carbonization of sucrose impregnated in the pores of MCM-48. The XRD patterns of MCM-48 after complete carbonization within the pores is similar to that of MCM-48 except for

slight changes associated with lattice contraction and intensity loss. According to Ryoo *et al.* [5], the lattice contraction usually results from high temperature heating of MCM-48 even without sucrose, whereas the pore filling with carbon can cause the intensity loss. The later evidence shows that both enantiomeric channel systems, separated by the silica walls corresponding to periodic G-surface (gyroid surface), are statistically equally filled with carbon, maintaining the cubic $Ia3d$ space group with inversion centers on the original G-surface. When the silica walls were removed, producing sample CMK-1, a new peak corresponding to the position of the (110) reflection for $Ia3d$ appears. The (110) reflection is symmetry forbidden for $Ia3d$. This result shows that there is a systematic transformation to a new ordered structure when silica walls were removed to allow the observation of the (110) reflection.

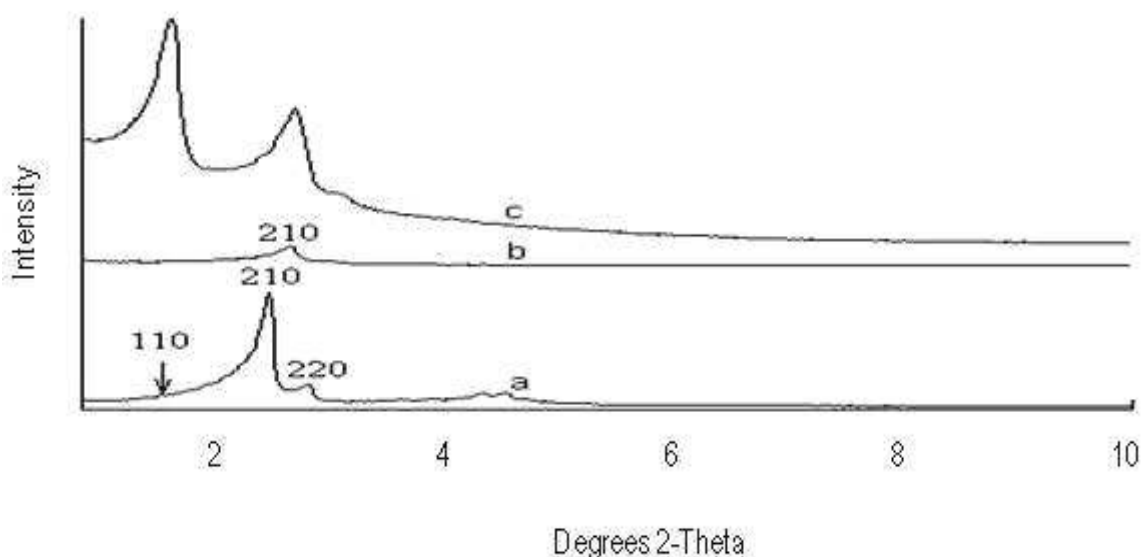


Fig. 1: Changes in XRD patterns during synthesis of mesoporous carbon from silica template, MCM-48. (a) MCM-48, (b) MCM-48 after completing carbonization within pores and (c) mesoporous carbon (CMK-1) obtained by removing silica wall after carbonization

One possibility for the new structure observed is cubic $I4_132$ [5]. Other information that can be observed in the XRD pattern of CMK-1 is that there are no Bragg lines observed in the region 2-Theta where is greater than 10° , showing that the carbon framework was atomically disordered. For comparison, XRD pattern of activated carbon (Norit SX 2) was also measured. There were no Bragg lines observed in the XRD pattern, showing that this material is amorphous. XRD measurements were also used to study the thermal stability of CMK-1 at various temperatures in air. It was found that CMK-1 was still stable after heating at 573 K, but the order of this material was less after heating at 623 K as shown in the decreasing intensity of the two Bragg lines.

The nitrogen adsorption isotherm of mesoporous carbon is presented in Figure 2 and for comparison, the isotherm of activated carbon (Norit SX2) is also included. The shape of isotherm for CMK-1 is of Type IV, whereas activated carbon (Norit SX2) has Type I shape with a hysteresis loop at $P/P^0 > 0.5$, which is a H4 type of hysteresis. The amount of nitrogen adsorbed in activated carbon at the high relative pressure is considerably smaller than that in CMK-1.

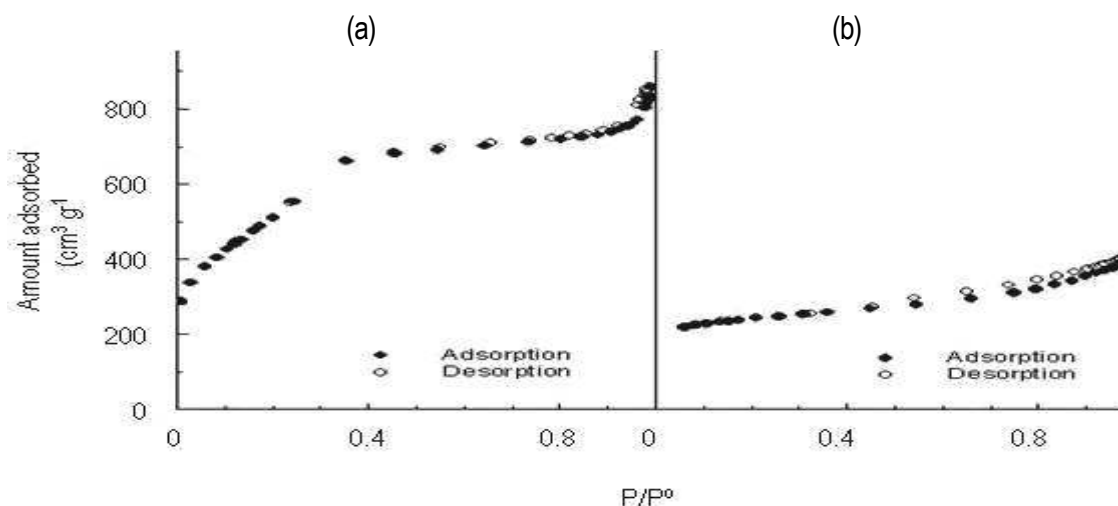


Fig. 2: Adsorption isotherms of (a) CMK-1 and (b) activated carbon (Norit SX 2)

Pore structure of CMK-1 together with MCM-48 and active carbon is given in Table 1. The BET surface area of CMK-1 is higher than that of activated carbon (Norit SX2). By comparing data of the pore structural properties of CMK-1 to the template MCM-48, it can be noted that the BET surface area of CMK-1 is 1.5 times higher than the template MCM-48. This large surface area of CMK-1 can be overestimated, which has been observed in previous studies [6, 8] by using the BET method.

Table 1: Pore structure parameters of CMK-1, MCM-48 and activated carbon (Norit SX2)

Samples	S_{BET} ($m^2 g^{-1}$)	S_{ex} ($m^2 g^{-1}$)	V_p ($cm^3 g^{-1}$)	V_t ($cm^3 g^{-1}$)	W_{BJH} (nm)	Wall thickness (nm)
CMK-1	1864.1 ± 16.8	167.64	0.96	1.29	2.95	1.24
Activated carbon (Norit SX2)	1103.6 ± 15.8	N/A	N/A	N/A	N/A	N/A
MCM-48	1230.7 ± 1.5	183.34	0.94	1.29	3.05	0.99

W_{BJH} was estimated from the BJH pore size distribution (adsorption branches) with the corrected form of the Kelvin equation for capillary condensation in cylindrical pores. Wall thickness was estimated using an equation proposed by Ravikovitch and Neimark; b (wall thickness) = $[1 - \{V_p \rho / (1 + V_p \rho)\}] (a_0 / x_0)$ where a_0 is the unit cell size taken from XRD experiment and x_0 is a constant, i.e. 3.0919. Uncertainty in $V_t = 0.05$ nm.

Figure 3(a) illustrates the water adsorption isotherm of CMK-1 together with the isotherm of activated carbon, and MCM-48 for comparison. The isotherm of CMK-1 is of Type V, the same as that of the template MCM-48, whereas activated carbon shows the Type III isotherm without any pore filling. At the low P/P^0 both CMK-1 and activated carbon only adsorbed a small amount of water vapor, indicating that the materials have hydrophobic features. The hydrophobicity of both materials is similar since the amount of water adsorbed at the low relative pressure is similar. The inflection point of CMK-1 is similar to that of the template MCM-48, which gives similar pore

diameter. The amount of water adsorbed at low P/P^0 in CMK-1 is slightly lower than that in the template MCM-48, indicating the former is slightly more hydrophobic than the latter.

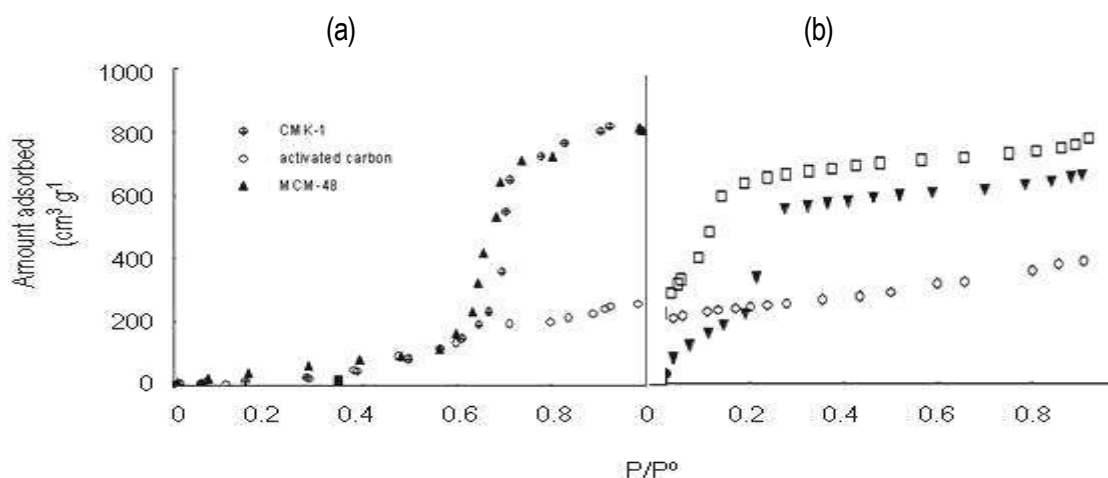


Fig. 3: Adsorption isotherm of CMK-1, activated carbon (Norit SX 2), MCM-48 for water (a) and benzene (b)

Benzene adsorption isotherms of CMK-1 and activated carbon together with the template MCM-48 and its modification are shown in Figure 3(b). The isotherm shape of CMK-1 is of Type IV, whereas activated carbon has a Type I isotherm. The amount of benzene adsorbed in CMK-1 is considerably higher than that in activated carbon, indicating that CMK-1 has a higher affinity to benzene than activated carbon. From Figure 3(b), it can be concluded that the adsorption capacities of benzene on the adsorbents at the low relative pressure follows the sequence of $\text{CMK-1} > \text{activated carbon} > \text{MCM-48}$.

Adsorption of dyes as a function of time

A study by XRD previously showed that CMK-1 was still stable after stirring for 5 h in water at room temperature and 373 K. Therefore a stirring method can be used for the adsorption of dyes from an aqueous solution. Before adsorption, an UV-visible wavelength maximum of reactive red 1 (RR1), rhodamine B (RhB), and patent blue V (PBV) was determined. It was found from spectra that there were 3 peaks found in the absorption spectrum of RR1 with the most intense at 510.5 and 532 nm. The wavelength of RR1 used for further experiments was 532 nm. There are 4 peaks observed for RhB, the most intense peak was found at 554 nm and it was used for further experiments. From 3 peaks observed in the absorption maximum PBV, the peak at 638 nm has the highest intensity. Therefore, this peak was used for measurement of the amount of PBV adsorbed from the solution.

Standard curves of dyes were obtained by measuring the absorbance of the dye solutions at the corresponding absorption maximum as a function of the solution concentration. The amount of dyes adsorbed was calculated by measuring the concentration of the dyes in the solution before and after adsorption.

To obtain the optimum period of time for adsorption, stirring of CMK-1 in dye solution was carried out for different periods of time. The change of the adsorbed amounts of RR1, RhB and PBV with time is shown in Figure 4. It is clear that the amount of RR1 adsorbed in CMK-1 steeply increases with increasing time and reaches plateau values within 120 min. The same trend was

observed when CMK-1 adsorbed RhB or PBV. On the basis of this result, the time used for determination of adsorption isotherms of these dyes was 120 min.

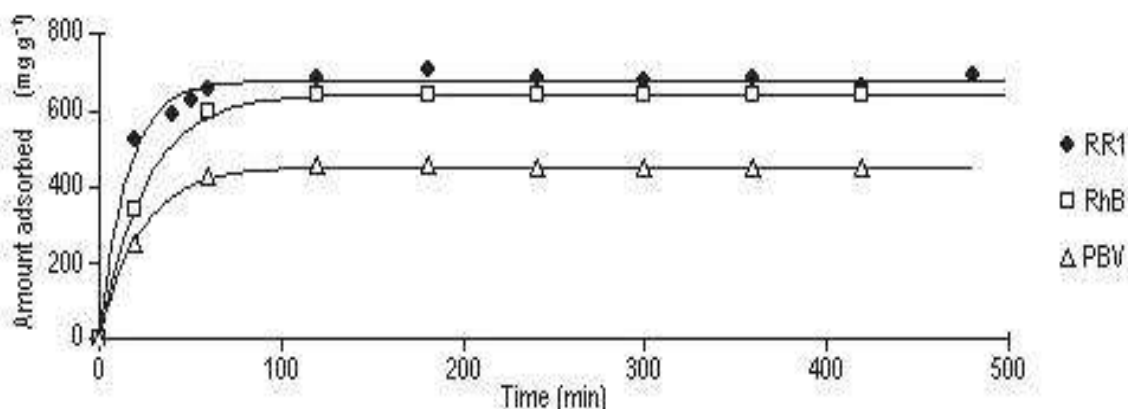


Fig. 4: Adsorption of Reactive Red I (RRI), Rhodamine B (RhB) and Patent Blue V (PBV) as a function of time (Initial dye concentration 300 mg L⁻¹)

Adsorption Isotherms of Dyes

The adsorption isotherms of dyes both in mesoporous carbon and activated carbon (Norit SX 2) were presented using Langmuir and Freundlich equations. The Langmuir isotherm assumes monolayer adsorption onto a surface containing a finite number of adsorption sites of uniform energies of adsorption with no transmigration of adsorbate in the plane of the surface. The Langmuir equation is given in the linear form as [9]:

$$\frac{C_e}{q_e} = \frac{1}{Q_0 b} + \frac{C_e}{Q_0} \quad (2)$$

where C_e (mg L⁻¹) is the equilibrium concentration of dye, q_e is the amount of dye adsorbed at equilibrium concentration (mg g⁻¹), Q_0 and b are the Langmuir constants related to the capacity and energy of adsorption, respectively. The constant Q_0 and b can be obtained from the intercept and slope of the linear plots of C_e/q_e Vs C_e .

The Freundlich isotherm model depends on an assumption of heterogeneous surface energies, where the energy term in the Langmuir equation varies as a function of the surface coverage. The linear form of this isotherm is given in equation 3 [9].

$$\log\left(\frac{X}{m}\right) = \log K + \left(\frac{1}{n}\right) \log C_e \quad (3)$$

where X is the amount of dye adsorbed (mg), m is the weight of the adsorbent used (g), C_e is the equilibrium concentration of dye solution (mg L⁻¹). K and n are Freundlich constants. K and n can be determined from the intercept and slope of the linear plot of $\log(X/m)$ Vs $\log(C_e)$.

Adsorption of Reactive Red-1 (RR1)

Figure 5 displays adsorption isotherms of RR1 in CMK-1 and activated carbon (Norit SX 2). The isotherm of this dye in MCM-48 is also presented for comparison. The amounts adsorbed are

expressed as mmol per m² of surface area. From this figure, it is clear that the amount of RR1 adsorbed in CMK-1 at certain concentration is considerably higher than that in activated carbon (Norit SX 2). The surface area and pore volume of CMK-1 (measured by nitrogen adsorption) are about twice those of activated carbon, so that the difference between the two forms of carbon is even more pronounced when adsorption is expressed per gram of adsorbent. The amount of RR1 adsorbed in MCM-48 is extremely small as shown in Figure 5(c). One explanation for this is that MCM-48 has less organophilicity than CMK-1 and also the former contains silanol groups, which can interact with water by hydrogen bonding. The hydrogen bonding between silanol groups and water may be considerably stronger than the hydrophobic interaction between MCM-48 and RR1.

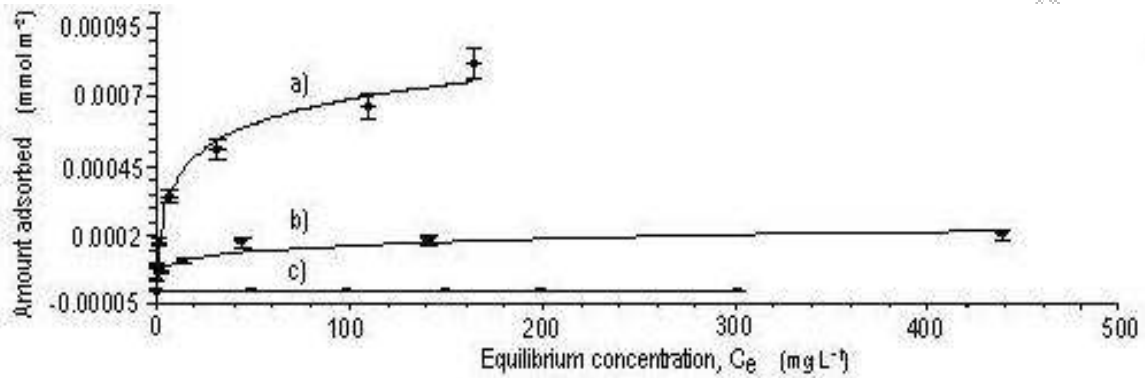


Fig. 5: Adsorption of (a) Reactive Red I (RRI), (b) Rhodamine B (RhB) and (c) Patent Blue V (PBV) as a function of time (Initial dye concentration 300 mg L⁻¹)

Figure 6 shows the Langmuir plots of RR1 in CMK-1 and activated carbon (Norit SX 2). The Langmuir constants of RR1 in CMK-1 and activated carbon are presented in Table 2. It can be seen that the Langmuir adsorption capacity (mmol m⁻²) of RR1 in CMK-1 is 4.1 times higher than that of RR1 in activated carbon (Norit SX 2). The Freundlich plots of RR1 in CMK-1 and activated carbon are displayed in Figure 7. Linear plots of log (X/m) against log C_e show that the adsorption of RR1 in both CMK-1 and activated carbon also appears to follow the Freundlich equation. However the fit to this model is significantly inferior to that of the Langmuir model, as judged by the correlation coefficients.

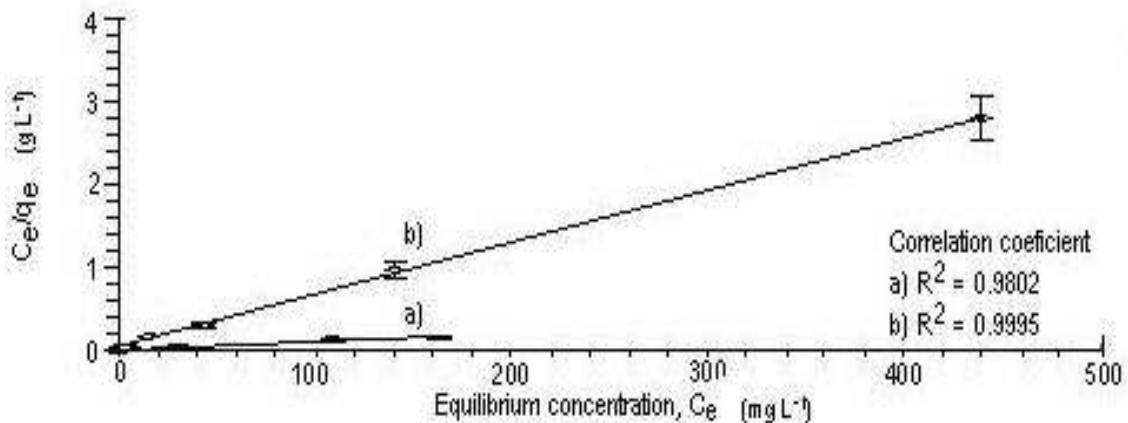


Fig. 6: Adsorption isotherms of RR1 in (a) CMK-1, (b) activated carbon (Norit SX 2) and (c) MCM-48

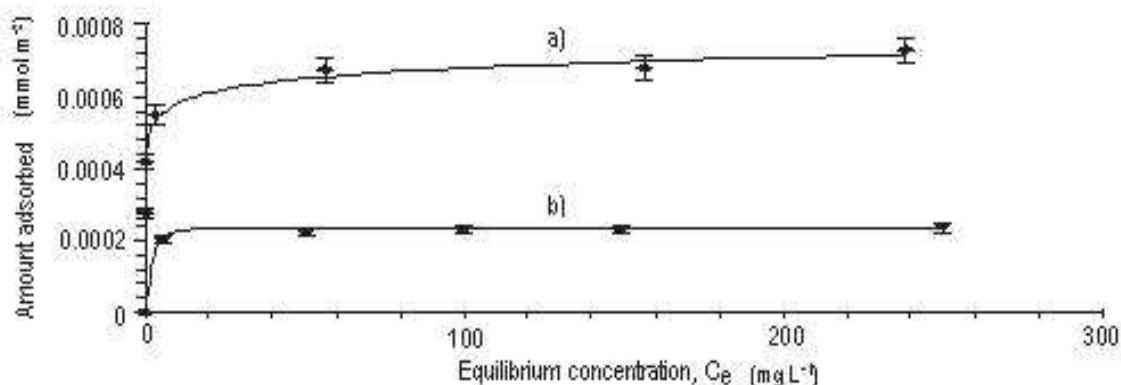


Fig. 7: Freundlich plots of RR1 in (a) CMK-1 and (b) activated carbon.

Table 2: Langmuir and Freundlich constants of RR1 in CMK-1 and activated carbon.

Adsorbent	Surface area (m ² g ⁻¹)	Q ₀		b (L mg ⁻¹)	K	n
		mg g ⁻¹	mmol m ⁻²)			
CMK-1	1864.1	1090.75	8.2 x 10 ⁻⁴	188.8	2.82	0.982
Activated carbon	1103.6	159.95	2.0 x 10 ⁻⁴	46.99	4.49	0.103

*) Calculated by dividing the amount of dye adsorbed by molecular mass of RR1 (717.37) and the surface area of adsorbents

Table 2 presents Freundlich constants of RR1 in CMK-1 and activated carbon. According to Namasivayam *et al.* [9], the adsorption capacity of the adsorption for a given dye increases with increasing K value. Therefore the adsorption capacity of RR1 in CMK-1 is higher than that in activated carbon, as was also concluded from the Langmuir isotherms.

Adsorption of Rhodamine B, RhB (Basic Dye)

Figure 8 shows adsorption isotherms of RhB in CMK-1 and activated carbon. As can be seen for RR1 adsorption, the amount of this dye adsorbed in CMK-1 at any given concentration is considerably higher than that in activated carbon. The Langmuir plots of the dye in both adsorbents are presented in Figure 9 and the Langmuir constants are summarized in Table 3. The adsorption capacity (mmol/cm²) of RhB in CMK-1 is higher than that of RhB in activated carbon by a factor of 3. Freundlich plots of RhB in CMK-1 and activated carbon can be seen in Figure 10. The adsorption capacity of RhB in CMK-1 is higher than that of RhB in activated carbon as can be seen from the values of K (Table 3).

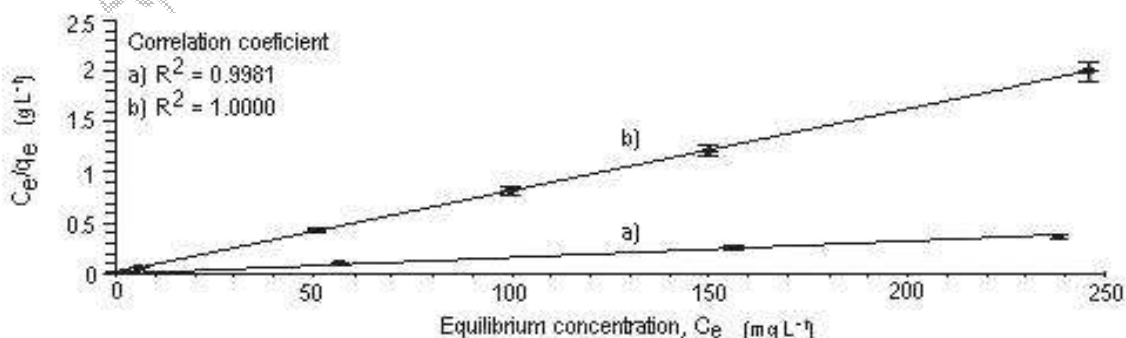


Fig. 8: Adsorption isotherms of RhB in (a) CMK-1 and (b) activated carbon (Norit SX 2)

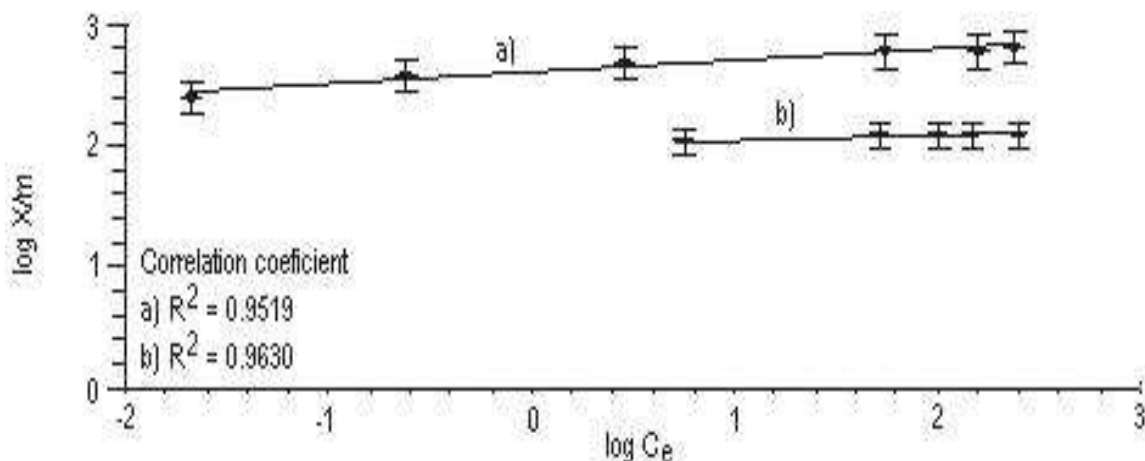


Fig. 9: Langmuir plots of RhB in (a) CMK-1 and (b) activated carbon (Norit SX 2)

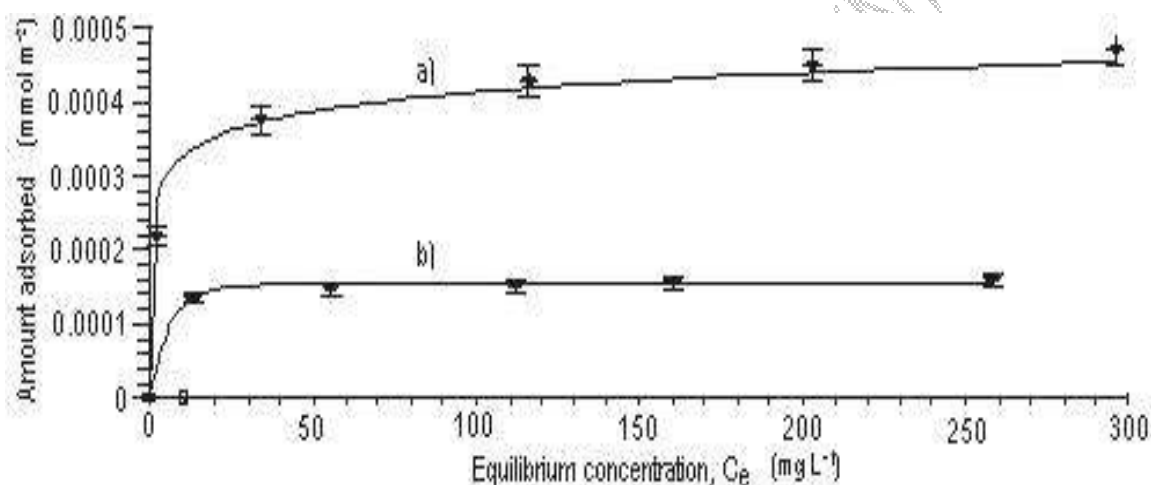


Fig. 10: Freundlich plot of RhB in (a) CMK-1 and (b) activated carbon (Norit SX 2)

Table 3: Langmuir and Freundlich constants of RhB in CMK-1 and activated carbon.

Adsorbent	Surface area (m ² g ⁻¹)	Q ₀		b L mg ⁻¹	K	n
		mg g ⁻¹	mmol m ^{-2*}			
CMK-1	1864.1	641.44	7.2 x 10 ⁻⁴	398.11	10.41	0.586
Activated carbon	1103.6	124.36	2.4 x 10 ⁻⁴	102.9	26.9	0.681

*Calculated by dividing the amount of dye adsorbed by molecular mass of RhB (479.02) and the surface area of adsorbents

Adsorption of Patent Blue V, PBV (Acid Dye)

Figure 11 represents adsorption isotherms of PBV in CMK-1 and activated carbon. As for RR1 and RhB, the amount of PBV adsorbed in CMK-1 is higher than that adsorbed in activated carbon. The Langmuir and Freundlich plots of the adsorption of PBV in CMK-1 and activated carbon are given in Figure 12 and Figure 13, respectively. Table 3 gives the Langmuir constants and the Freundlich constants of the PBV adsorption in both adsorbents. The adsorption capacity (mmol cm⁻²) of PBV in CMK-1 is 3 times higher than that of PBV in activated carbon. Figure 13 also shows that the adsorption capacity of PBV in CMK-1 is higher than in activated carbon.

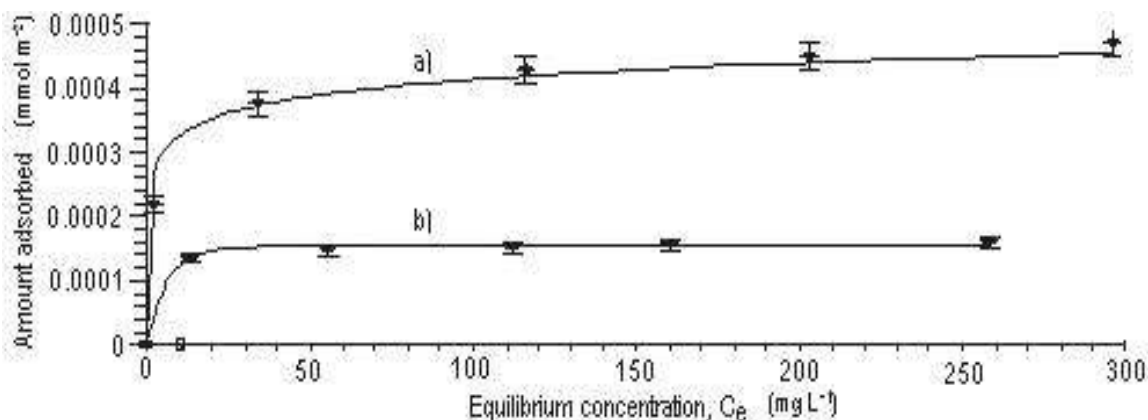


Fig. 11: Adsorption isotherm of PBV in (a) CMK-1 and (b) activated carbon (Norit SX 2)

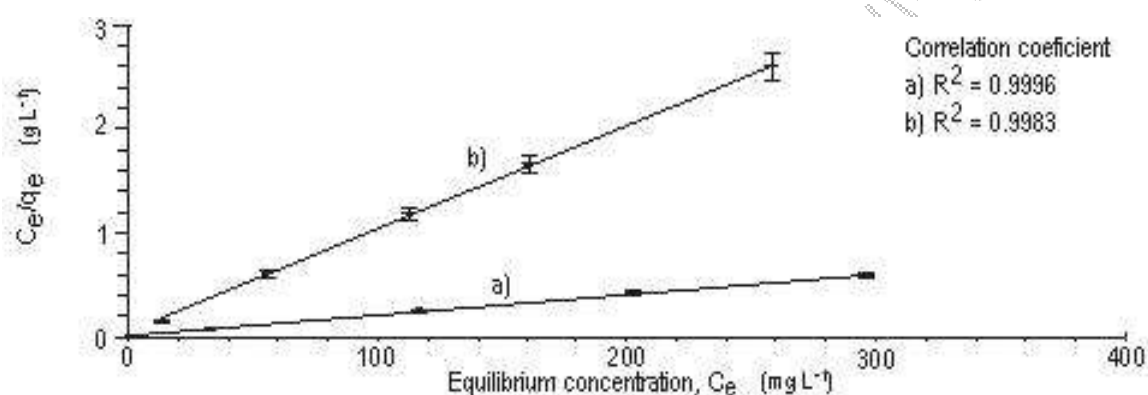


Fig. 12: Langmuir plots of PBV in (a) CMK-1 and (b) activated carbon (Norit SX 2)

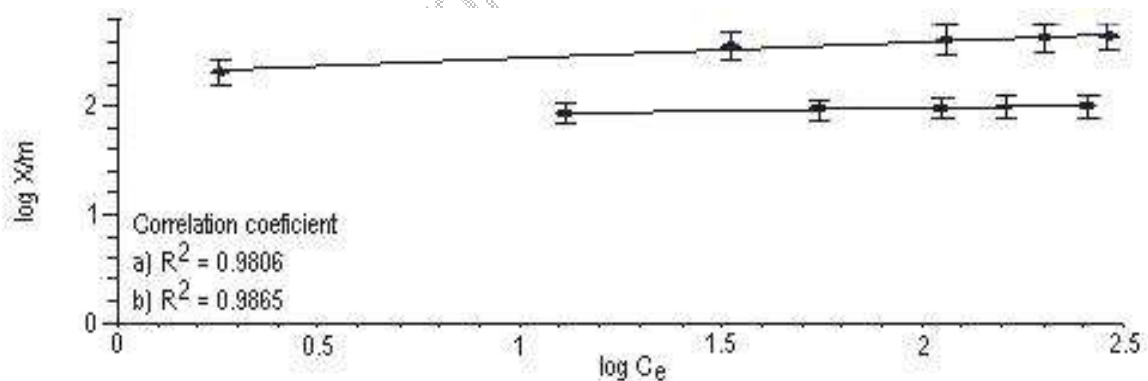


Fig. 13: Freundlich plots of PBV in (a) CMK-1 and (b) activated carbon (Norit SX 2)

Table 3: Langmuir and Freundlich constants of PBV in CMK-1 and activated carbon.

Adsorbent	Surface area (m ² g ⁻¹)	Q ₀		b L mg ⁻¹	K	n
		mg g ⁻¹	mmol m ⁻² *			
CMK-1	1864.1	503.27	4.8 x 10 ⁻⁴	0.130	217.77	6.62
Activated carbon	1103.6	100.59	1.6 x 10 ⁻⁴	0.207	74.47	19.47

*) Calculated by dividing the amount of dye adsorbed by molecular mass of PBV (566.66) and the surface area of adsorbents

CONCLUSIONS

The adsorption of the three dyes in CMK-1 and activated carbon can be fitted to both the Langmuir and Freundlich models, although with the possible exception of RR1 in activated carbon, better fits are obtained with the Langmuir model. The fraction of the surface area accessible to RR1, RhB and PBV in CMK-1 was considerably higher than that in activated carbon. For the smaller molecule, benzene, the fraction of the surface area accessible to the molecule is the same for both CMK-1 and activated carbon. This can be explained by the fact that activated carbon has a lot of micropores which benzene can fit in but the dye molecules cannot, whereas CMK-1 does not.

Acknowledgements: This work was financed by Australian Agency for International Development (AusAID).

References

1. Reife, A. and H.S. Freeman, 1996. Environmental Chemistry of Dyes and Pigments, John Wiley & Sons, INC, New York.
2. McKay, G., Elgeundi, M. and M.M. Nassa, 1996. Pore Diffusion during the Adsorption of Dyes onto Bagasse Pith. *Process Safety and Environmental Protection*, 74: 277-280.
3. Tamai, H., Yoshida, T., Sasaki, M. and H. Yasuda, 1999. Dye adsorption on mesoporous activated carbon fiber obtained from pitch containing yttrium complex. *Carbon*, 37: 983-989.
4. Walker, G. M. and L.R. Weatherley, 2000. Prediction of bisolute dye adsorption isotherms on activated carbon. *Process Safety and Environmental Protection*, 78: 219-223.
5. Ryoo, R., Joo, S. H. and K.J. Kim, 1999. Synthesis of Highly Ordered Carbon Molecular Sieves via Template-mediated Structural. *Journal of Physical Chemistry B*, 103: 7743-7746.
6. Kruk, M., Jaroniec, M., Ryoo, R. and S.H. Joo, 2000. Characterization of Ordered Mesoporous Carbon Synthesized using MCM-48 Silica as Templates. *Journal of Physical Chemistry B*, 104: 7960-7968.
7. Vinu, A., Hossain, K. Z., Kumar, G. S. and K. Ariga, 2006. Adsorption of L-histidine over Mesoporous Carbon Molecular Sieve. *Carbon*, 44: 530-536.
8. Baratta, G.A., Arena, M.M., Strazzulla, G., Colangeli, L., Mennella, V. and E. Bussoletti, 1996. Raman Spectroscopy of ion irradiated amorphous carbons. *Nuclear Instruments and methods in Physics Research Section B*, 116: 195-199.
9. Namasivayam, C., Radhika, R. and S. Suba, 2001. Uptake of dyes by a promising locally available agricultural solid waste: coir pith. *Waste Management*, 21: 381-387.